Membranes:
quasi-2D complex fluid embedded in 3D

Cells and cellular organelles are enveloped by membranes, whose main structural component is a lipid bilayer.

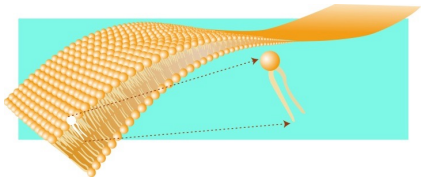

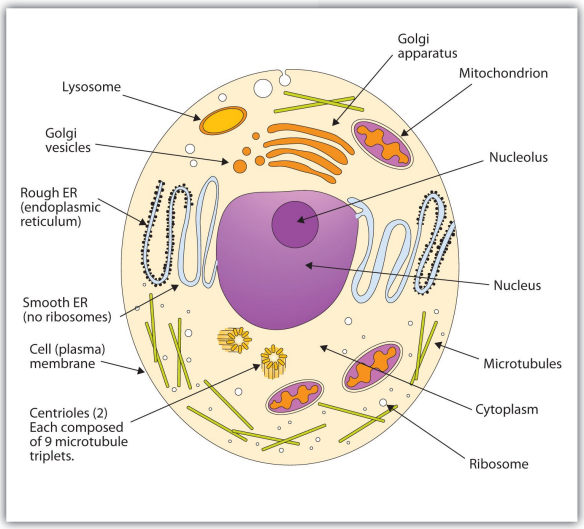

"demands"

1. isolate cell content; sequester functions
2. selective permeability
3. malleable topology

https://www.cmu.edu/biolphys/deserno/pdf/membrane_theory.pdf

1

Biomembranes: deformation

trafficking

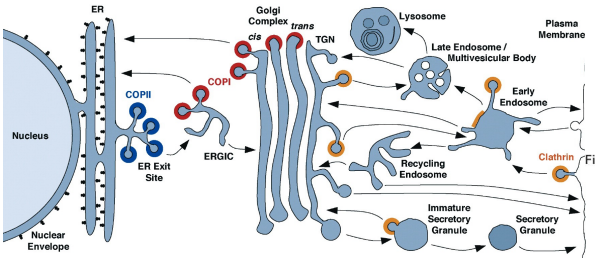

Bonifacino and Glick, Cell (2004)

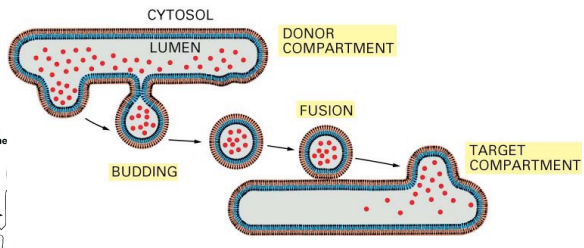

Figure 13–2. Molecular Biology of the Cell, 4th Edition.

mechanotransduction

neurotransmission

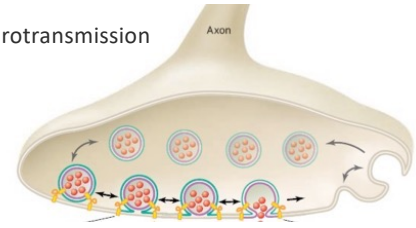

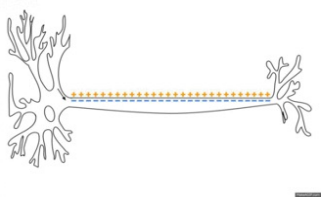

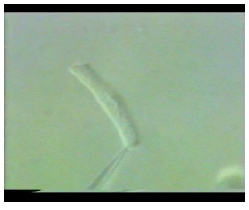

Zimmerberg and Chernomordik, Science (2005)

http://www.physiol.ucl.ac.uk/ashmore/

2

Cell membranes: structured interfaces (complex 2D fluid)

Membranes are constantly deformed

From the "Inner Life of the Cell"

Membranes are multicomponent

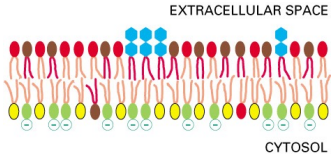

Figure 10–14. Molecular Biology of the Cell, 4th Edition.

Membranes are fluid

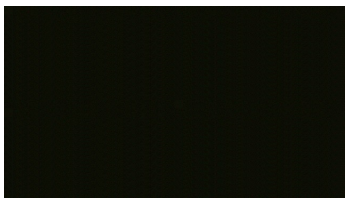

Membranes are charged

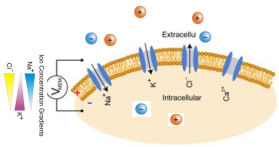

(bound charge)

(mobile charges)

membranes "store" charge:
transmembrane potential ~100mV

$$Q = C_m V_m$$

C_m~ 1 μF/cm^2

Electric field
in the membrane:

$$E_m = \frac{V_m}{d} \sim 10\ \text{MV/m}$$

3

Outline

- Composition of biomembranes
  - amphiphiles
- Self assembly of amphiphiles
  - CMC (critical micelle concentration)
  - Shape of molecule in relation to structure of aggregate
- Bilayer mechanics
  - • compression resistance
    - the lipid bilayer is a 2D- incompressible fluid
  - • bending resistance
    - ~few kT
- Shapes of closed membranes: why is the RBC a biconcave disk?
- Fluctuations and deformations

RBC/vesicle flicker

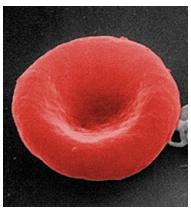

https://www.youtube.com/watch?v=VwhNLaRCD-4

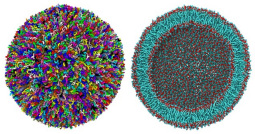

Matti Javanainen
(Tampere, Finland)
Balasz Fabian
(MPI, Germany)

RBC/vesicle in flow

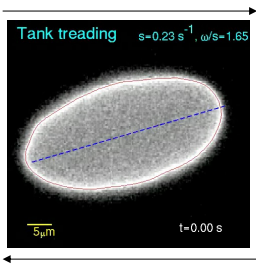

4

Biomembranes

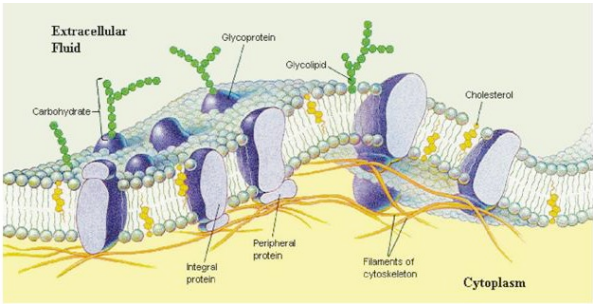

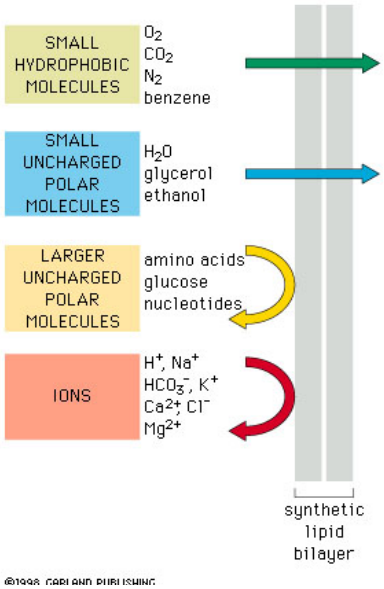

- 2-molecule thick structure (5nm), held together by non-covalent bonds
- dynamic fluid structures (molecular motion)
- lipid bilayer:
  - semipermeable barrier, sealant
  - provides 2D solvent for membrane proteins

5

Membrane composition

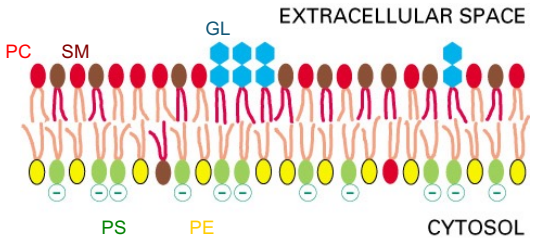

Figure 10–14. Molecular Biology of the Cell, 4th Edition.

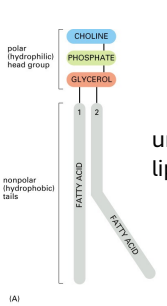

Figure 10-2 part 1 of 3. Molecular Biology of the Cell, 4th Edition.

unsaturated lipid

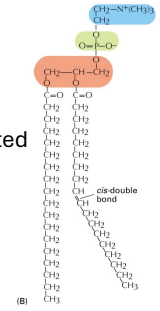

Figure 10-2 part 2 of 3. Molecular Biology of the Cell, 4th Edition.

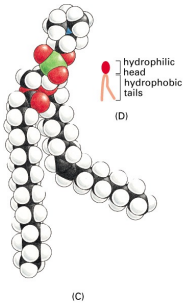

Figure 10-2 part 3 of 3. Molecular Biology of the Cell, 4th Edition.

Lipids are example of amphiphilic molecules

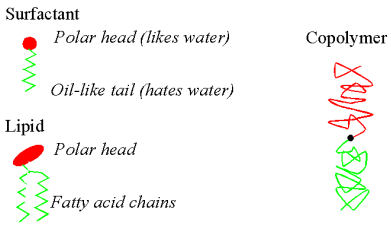

Lipid bilayers are example of self-assembled structures

6

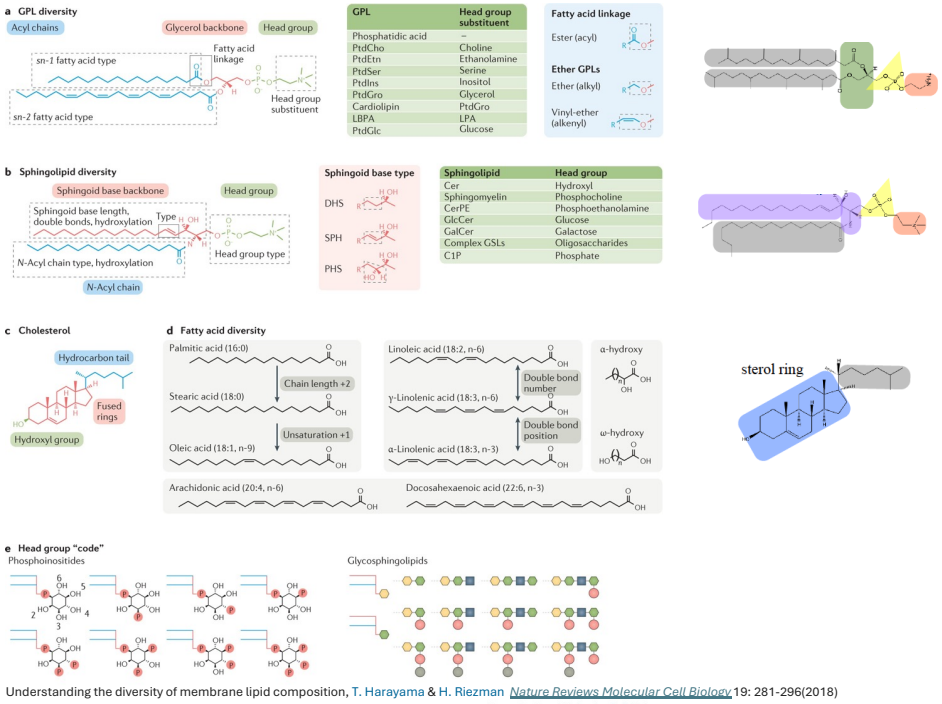

Understanding the diversity of membrane lipid composition, T. Harayama & H. Riezman *Nature Reviews Molecular Cell Biology* 19: 281-296(2018)

Nature Reviews | Molecular Cell Biology

7

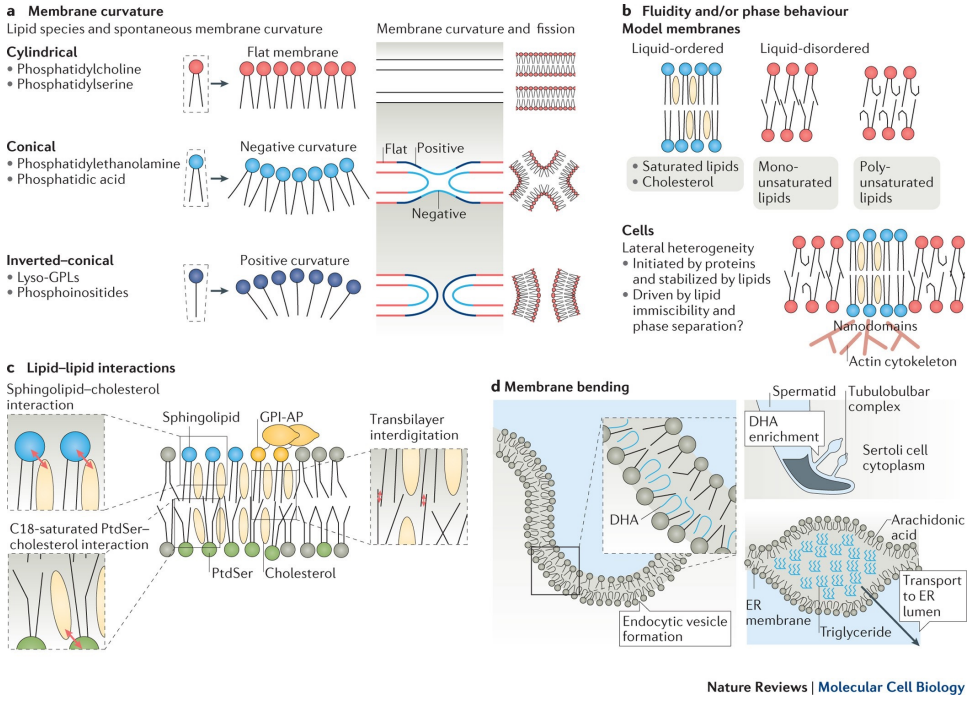

Nature Reviews | Molecular Cell Biology

8

Surfactants

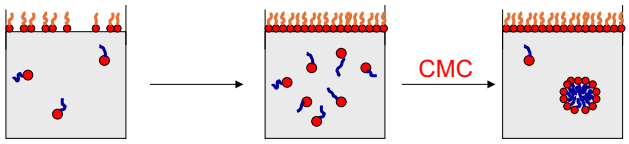

Driving force: the hydrophobic effect

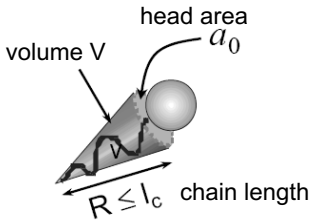

Packing parameter (shape factor):

$$p = \frac{V}{a_o l_c}$$

Self assembly of amphiphiles: Different forms of aggregates

spherical micelles : p<1/3

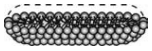

non-spherical micelles : 1/3<p<1/2

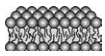

bilayers and vesicles: ½<p<1

small head-group
and bulky chains

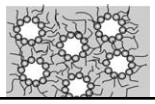

inverted micelles: p>1

9

Why are membranes made of lipids?

Two chains ⇒ 1) hydrophobicity ↑ ⇒ CMC ↓
CMC micelle formation 10^{-2}-10^{-5} M
CMC bilayer formation 10^{-6}-10^{-10} M
2) residence time ~ probability for a molecule to leave the aggregate
t~1/CMC
micelles 10^{-4} s
bilayer 10^{4} s
3) flip-flop times ~ exp(E/kT) E: enery to put the hydrophilic head in the hydrophobic core
10^{2}-10^{5} s

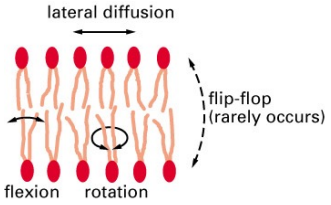

Figure 10–8. Molecular Biology of the Cell, 4th Edition.

10

Membrane mechanics

Elasticity: bending rigidity (Helfrich/Willmore –no structure)

$$E = \int dS \left(2\kappa H^2 + \kappa_G K\right)$$

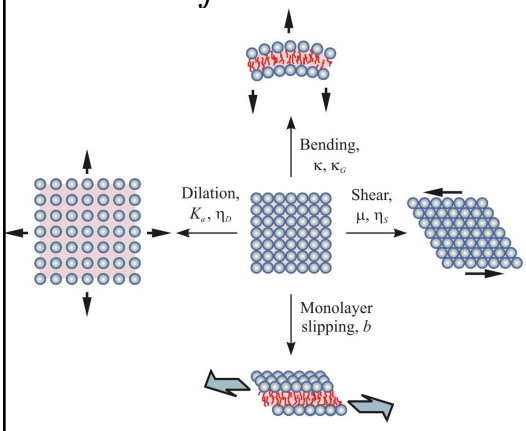

Dissipation:

- inter-monolayer friction (bilayer slip)

$$P_b = \int dS \frac{b}{2} \left(\mathbf{v}^+ - \mathbf{v}^-\right)^2$$

- in-plane flow (incompressible 2D Newtonian fluid) membrane viscosity

$$P_s = \int dS \left(\eta_s \mathbf{d} : \mathbf{d}\right)$$

Boussinesq–Scriven model $\mathbf{d} = \frac{1}{2}\left(\nabla_s \mathbf{v} + \nabla_s \mathbf{v}^T\right) + v_n \nabla_s \mathbf{n}$

Rahimi et al. Soft Matter (2013)
Fournier Int. J. Non-lin. Mech. (2015)

Dimova et al. J. Phys. Cond. Mat. (2006)

11

Bilayer bending resistance

Interpretation of bending modulus:

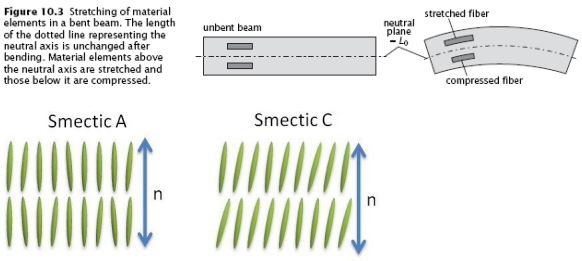

Bending of a bilayer = stretching of one leaflet and compression of the other leaflet

$$\kappa_b = \frac{K_A d^2}{\alpha}$$

α=12 for a plate that can not slide
α=48 for a plate that can slide
α=24 for the polymer brush model

Bending of a bilayer = splay

Bilayer compression

Approach from elasticity theory *neglects* rearrangement of lipids in response to stress,

Surface tension theory ⇒ $K_A = 4\gamma$ for bilayer

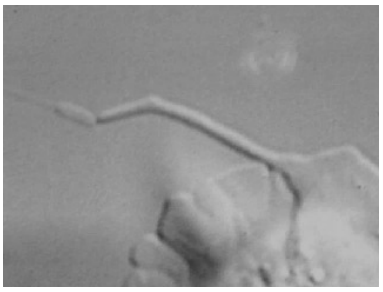

12

Equilibrium shapes

"energy" approach

$$E = \frac{\kappa}{2}\int H^2 dA + \sigma A + pV + \int \kappa_G K \, dA$$

constant area — constant volume

here $H = \nabla \cdot \mathbf{n}$

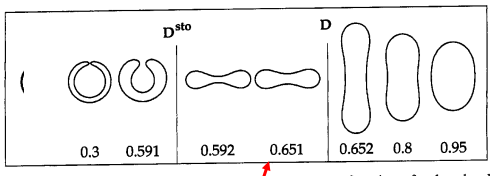

Figure 14. Energy G and contours of stationary shapes as a function of reduced volume v. All shapes have the same area. D and D^{sto} denote the discontinuous prolate/oblate and oblate/stomatocyte transition. The oblates and the stomatocytes lose metastability at C^{sto} and M^{sto}, respectively. Beyond the diamond, the oblates self-intersect (Seifert *et al* 1991).

Seifert, *Adv.Phys.* 46 (1997)

RBC: reduced volume =0.64

Reduced volume

$$v = \frac{V}{\frac{4\pi}{3}\left(\frac{A}{4\pi}\right)^{3/2}}$$

"mechanical" approach

$$p^{in} - p^{out} = -\kappa\left[4H^3 - 4HK + 2\nabla_s^2 H\right] + 2\sigma H$$

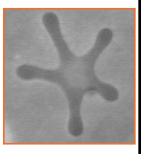

more complex shapes- spontaneous curvature, multicomponent membranes

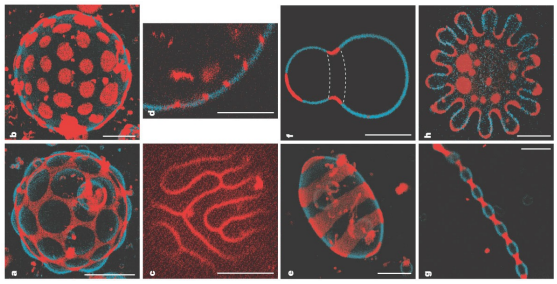

Baumgart et al. "Imaging coexisting fluid domains in biomembrane models coupling curvature and line tension" Nature (2003) 425:821–824

13

13

How to compute shapes?

(see notes for references)

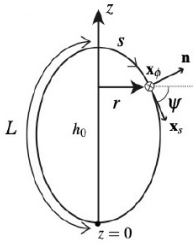

$$c_1 = r_s z_{ss} - z_s r_{ss}$$

$$c_2 = \frac{z_s}{r}$$

see Reboucas et al "Stationary shapes of axisymmetric vesicles beyond lowest-energy configurations" Soft Matter, 2024

about how to solve for the shapes. The Appendix also shows how to derive the "mechanical" equilibrium equations from the Helfrich energy.

$$2\kappa\Delta_b H + 4\kappa H(H^2 - K) - 2H\Sigma - P = 0$$

$$(r_s)^2 + (z_s)^2 = 1$$

$$r(0) = 0, \qquad r(L) = 0$$

$$z_s(0) = 0, \qquad z_s(L) = 0$$

at the poles $H_s = 0$

14

On membrane tension …

At this stage, it seems that surface tension is a superfluous concept for vesicles. Their conformations rather live in the "conjugated" ensemble where the area is constrained. Still, there has been some confusion about surface tension of membranes mostly due to the lack of a sensible definition of surface tension in such a system. The folklore includes statements like "the surface tension vanishes due to the fact that each molecule has its preferred area" or "the surface tension is practically infinite since membranes are so hard to stretch." While the former can be justified in the sense that the area can adjust optimally to its preferred value, the latter statement is nonsense even though membranes are comparatively hard to stretch indeed. Physical insight is contained in the idea that "the area constraint implies an [illegible]"

Seifert "The concept of effective tension for fluctuating vesicles", Z. Phys. (1995)

For liquid interfaces, the surface tension is a constant depending only on the nature of the phases in contact. The situation for membranes is quite different. Membranes consist of a fixed number of insoluble lipids possessing an equilibrium density. Mechanically, the tension depends on the lipid density but also on the curvature of the membrane [8–10]. Nonetheless, for fluid membranes, the concept of surface tension is threefold: i) Experimentally, one measures a tension τ from the quadratic dependence in the wave number of the fluctuation spectrum [2]. ii) Theoretically, one can introduce in the Hamiltonian a Lagrange multiplier σ multiplying the total membrane area. In principle τ can be deduced from σ by renormalization procedures [11,12]. (More accurately, one may fix the total membrane area by a constraint [13] or, even better, keep the lipid density as a parameter [8].) iii) Experimentally, one measures another tension, τ, through the pressure difference across the membrane by means of the Laplace relation [14,15]. In principle, this is the actual (macroscopic) tension, since it corresponds to the average force that is exerted tangentially to the average membrane's surface. In principle, τ can be calculated by differentiating the total free energy with respect to the projected area [12], but this is a tricky matter [16]. The confusion associated with these different tensions inspired many articles [11,12,16–21].

Barbetta et al, "On the surface tension of fluctuating quasi-spherical vesicles". Eur. Phys. J. E (2010)
Criticism by Schmidt "Are stress-free membranes really "tensionless"?", EPL (2011)

15

Bilayer fluidity varies with temperature …

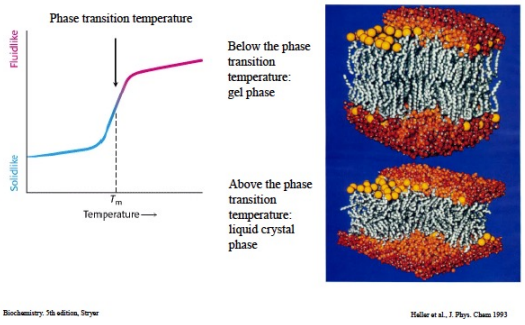

.. and composition: Lipid rafts

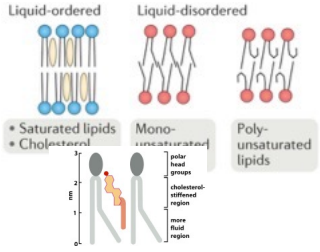

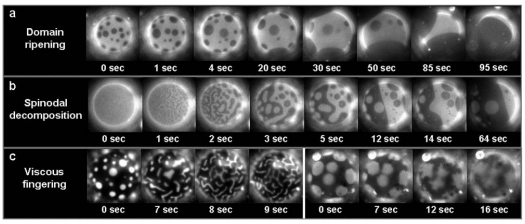

FIGURE 3 Giant vesicles observed near the miscibility transition. (a) Domain ripening through time in a vesicle of 1:1 DOPC/DPPC125% Chol. Although the proportion of dark phase increases in one hemisphere, it is roughly constant in time over the entire vesicle. (b) Time sequence suggesting spinodal decomposition in a vesicle of 1:1 DOPC/DPPC 1 35% Chol. (c) Viscous fingering in a vesicle of 1:9 DOPC/DPPC 1 25% Chol (left series) and 1:1 DOPC/ DMPC 1 25% Chol (right series) as temperature is raised through the miscibility transition. The uniform stripe-widths shown at the left are unique to this vesicle composition. All vesicles are roughly 30 microns in diameter.

Veatch and Keller …

.. and electric fields

16

PNAS, 2005

On soliton propagation in biomembranes and nerves

Thomas Heimburg* and Andrew D. Jackson

The Niels Bohr Institute, University of Copenhagen, 17 Blegdamsvej, 2100 Copenhagen Ø, Denmark

Communicated by Gordon A. Baym, University of Illinois at Urbana–Champaign, Urbana, IL, May 9, 2005 (received for review February 14, 2005)

The lipids of biological membranes and intact biomembranes display chain melting transitions close to temperatures of physiological interest. During this transition the heat capacity, volume and area compressibilities, and relaxation times all reach maxima. Compressibilities are thus nonlinear functions of temperature and pressure in the vicinity of the melting transition, and we show that this feature leads to the possibility of soliton propagation in such membranes. In particular, if the membrane state is above the melting transition solitons will involve changes in lipid state. We discuss solitons in the context of several striking properties of nerve membranes under the influence of the action potential, including mechanical dislocations and temperature changes.

It is less known that melting transitions can also be found in biological membranes, e.g., in *Escherichia coli* and *Bacillus subtilis* membranes (this work) and lung surfactant (3), which exists on the lung surface as a monolayer–bilayer equilibrium. In these systems the intact membranes, including all proteins, display pronounced lipid melting peaks slightly below physiological temperature (see Fig. 1). In the *E. coli* system the lipid melting peak changes with growth temperature and pH. It would be of importance to understand how the adaptable lipid composition influences the physical features of the membranes. Unfortunately, the lipid and protein composition of biomembranes is so diverse that it is seemingly impossible to understand the corresponding phase diagrams in detail. It is clear, however, that even these complex systems are

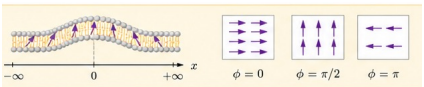

Summary: A smectic-C soliton in a single lipid bilayer is a localized deformation in which the in-plane director rotates by π across a finite distance, while the bilayer bends (splays) but remains continuous with approximately constant thickness d.

PHYSICAL REVIEW E VOLUME 51, NUMBER 4 APRIL 1995

Solitons in cell membranes

Pradip Das and W. H. Schwarz

Institute for Biophysical Research on Macromolecular Assemblies, The Johns Hopkins University, Baltimore, Maryland 21218

(Received 28 June 1993; revised manuscript received 4 November 1994)

Using a two-dimensional smectic liquid crystal model, we have shown the plausibility of electrical solitary wave propagation along a bimolecular leaflet such as the cell membrane of a nerve axon which consists of chiral, lipid building blocks. Our model is a head-to-tail correlated ferroelectric, chiral Sm-C^* liquid crystal, which is a unique class of substances that combines the electric polarization and anisotropy of ferroelectric crystals with the hydrodynamic properties of liquids. Polar Sm-A models can also be used with the same results. In addition to the usual transverse ferroelectricity, characteristic of the Sm-C^* liquid crystal, the head-to-tail correlation ensures a longitudinal ferroelectricity component. The electric polarization due to the latter can couple to the transmembrane electric field resulting from the ionic imbalance between the two sides of the membrane—a mechanism detailed in the so-called Hodgkin-Huxley set of partial differential equations for the propagation of the action potential. We obtain a Landau–de Gennes–like free energy, which is the sum of elastic, fluctuation, and polarization terms, together with a ferroelectric term showing a direct coupling between the electric field and the mechanical deformation variable. Minimizing and equating to a viscous damping term leads to an equation similar to one equation of the Fitzhugh-Nagumo coupled set of partial differential equations, which is a simplified version of the Hodgkin-Huxley equations. The other equation of the set resembles an equation derived from the Nernst-Planck equation, which describes transmembrane ion transport and hence provides a mechanism for transmembrane potential variation. A more complete calculation of the velocity of the asymptotic wave form shows a lower wave speed than the estimate of Nagumo *et al.* The piezoelectric properties of the phase compete with its curvature elasticity to produce the soliton lattice of the cell membrane, which consists of juxtaposed regions of opposite tilt orientations. The propagation of the solitary wave requires a switching electric field, which is the form for the action potential and which moves the polarized domains by ferroelectric switching.

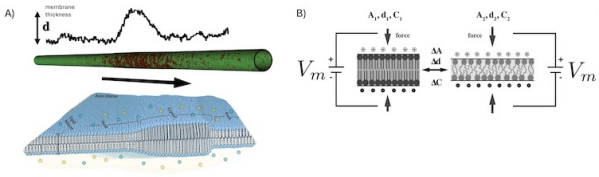

17

Note: the Helfrich model treats the membrane as a structureless zero-thickness interface. The Seifert-Langer model (1993, **DOI** 10.1209/0295-5075/23/1/012) includes contributions from the compression and expansion of the monolayers

see also Watson and Brown (J Phys Chem 2011), Miao et al. (EPJE, 2002), Vlahovska and Granek (Soft Matter, 2025)

$$E = \int dS \left(\frac{\kappa}{2}(2H)^2 + \frac{K_m}{2}\left[(\phi^- + 2dH)^2 + (\phi^+ - 2dH)^2\right] \right)$$

here $H = -\frac{1}{2}\nabla \cdot \mathbf{n}$

$\boldsymbol{\phi}^{\pm} = \boldsymbol{\rho}^{\pm}/\boldsymbol{\rho}_0 - \mathbf{1}$

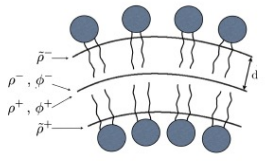

Fig. 1 Structure of a lipid membrane formed by two identical monolayers. At the bilayer neutral surface bending and stretching are decoupled. $\rho^{\mp}$ are the monolayers densities, $\tilde{\rho}^{\mp}$, projected onto the neutral surface. $\rho^{\mp} = \tilde{\rho}^{\mp}(1 \pm 2dH)$, where d is the monolayer thickness and H is the mean curvature.

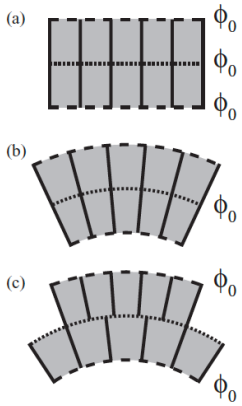

FIG. 4. (A) An undeformed bilayer, where the density at every surface is ϕ_0. Each rectangle represents a lipid. (B) When the membrane is suddenly bent, dissipative forces at the midplane (dotted) hinder the lipids from rearranging. Hence, the number densities at the midplane remain unchanged. (C) Over time, the lipids rearrange so that the minimal energy in the bent geometry is achieved, in which $\phi^{\pm} = \phi_0$ (dashed). Bilayer bending over short timescales is significantly more energetically costly than over longer timescales.

18